Journal of Quantitative Spectroscopy & Radiative Transfer 256 (2020) 107302

Contents lists available at ScienceDirect

Journal of Quantitative Spectroscopy & Radiative Transfer

journal homepage: www.elsevier.com/locate/jqsrt

Theoretical study of scattering Angstrom exponent of coated black carbon aerosols: The effect of microphysical configurations

Xiaolin Zhang[a,b,c,d], Mao Mao[a,c,*], Hongbin Chen[b], Shihao Tang[d]

[a] Key Laboratory of Meteorological Disaster, Ministry of Education (KLME) / Earth System Modeling Center (ESMC) / Collaborative Innovation Center on Forecast and Evaluation of Meteorological Disasters (CIC-FEMD) / Joint International Research Laboratory of Climate and Environment Change (ILCEC) / Key Laboratory for Aerosol-Cloud-Precipitation of China Meteorological Administration, Nanjing University of Information Science & Technology, Nanjing 210044, China

[b] Key Laboratory of Middle Atmosphere and Global Environment Observation (LAGEO), Institute of Atmospheric Physics, Chinese Academy of Sciences, Beijing 100029, China

[c] School of Atmospheric Physics, Nanjing University of Information Science & Technology, Nanjing 210044, China

[d] National Satellite Meteorological Center, China Meteorological Administration, Beijing 100081, China

ARTICLE INFO

Article history:
Received 20 March 2020
Revised 29 August 2020
Accepted 29 August 2020
Available online 30 August 2020

Keywords:
Black carbon aerosol
Scattering Angstrom exponent
Coating
Numerical investigation

ABSTRACT

The study numerically assesses the influences of particle microphysics, including shell/core ratio, black carbon (BC) geometry, coated volume fraction of BC, and size distribution, on the scattering Angstrom exponent (SAE) of polydisperse BC aggregates coated by organics based on the multiple-sphere T-matrix method. The dependence of coated BC scattering on shell/core ratio is highest among all microphysical parameters, indicating the significance of ambient measurements of BC shell/core ratio. The SAE of coated BC exhibits wavelength dependence with smaller value at smaller wavelength, whereas the SAE uncertainty due to wavelength selection is limited with differences less than 10%. The SAE values of coated BC between 450 nm and 700 nm have broad variation with a range of 0.5–2.6 for typical coated BC microphysics. The SAE of coated BC is highly sensitive to size distribution, and it decreases with particle becoming larger. Compared to size distribution, the dependence of the SAE on shell/core ratio, BC geometry, coated volume fraction of BC is generally weak, and the SAE of coated BC with larger coated volume fraction of BC becomes less sensitive to BC fractal dimension but more sensitive to shell/core ratio. The popular core-shell Mie model generally shows acceptable SAE results for heavily coated BC with differences within 10%, whereas significant SAE errors can be introduced for thinly coated BC particles. Our work clearly demonstrates the impact of particle size distribution on the SAE of coated BC based on more realistic BC geometries, yet suggesting that smaller SAE of coated BC may not always indicate larger particles, particularly for thinly coated BC aerosols.

1. Introduction

Aerosol particles from natural and anthropogenic sources, are common in the air and have important effects on the climate and environment [1,2]. As a significant contributor to global warming after CO_2, black carbon (BC) aerosols contribute important positive radiative forcing due to their strong absorption of solar radiation [3]. Meanwhile, BC tends to be coated by secondary aerosol species (e.g., organics and sulfate) through aging process and complicated internal-mixed particles are formed [4,5]. The resulting complex microphysical and optical properties of aged BC particles have been one of the largest uncertainties in assessing aerosol radiative forcing [6].

As one of aerosol optical properties, the Angstrom exponent is an important property utilized to express the dependence of any parameter (such as extinction, absorption or scattering) on incident wavelength. The extinction Angstrom exponent (EAE) is deemed to be related to particle size, and the values of EAE higher than 1 and lower than 1 indicate fine and coarse particles dominated, respectively [7]. The EAE is not a strict indicator of particle size, since it is also dependent on the absorption of aerosols [8]. The absorption Angstrom exponent (AAE) gives information on particle absorbing types, and it describes wavelength variation in particle absorption [9]. The AAE value close to 1.0 is referred as pure BC particles, and BC with non-absorbing coating can have AAE around 1.6 [10]. Meanwhile, the AAE shows dependence on wavelength

* Corresponding author.
E-mail addresses: xlnzhang@nuist.edu.cn (X. Zhang), mmao@nuist.edu.cn (M. Mao).

https://doi.org/10.1016/j.jqsrt.2020.107302
0022-4073/

ranges selected for the determination of its value [e.g., 9]. In addition to the EAE and AAE, the scattering Angstrom exponent (SAE) is applied to assess aerosol scattering of solar radiation, and its value is 4.0 in the Rayleigh regime [11]. Non-absorbing coatings on BC can enhance BC absorption through the well-known "lensing effect" that scattering material can focus more photons onto BC core [12]. BC shell/core ratio impacts the scattering and absorption of coated BC [13] and further its Angstrom exponents, and the sunglasses effect may also be an influence factor [14].

The SAE is regarded as a parameter describing particle size with small value indicating large size, and is considered to be in a range of 0.0–4.0. However, is aerosol SAE always only sensitive to its particle size? Does aerosol other microphysics (such as mixing state and morphology) also affect its SAE value under some circumstances? What is the typical value range of the SAE of aged BC aerosols, since more and more observations related to aged BC microphysics are presented recently? Meanwhile, the applicability of core-shell Mie model for the SAE of aged BC also needs to be evaluated, as it is widely used but debated for the obtainment of many optical properties of coated BC. To reply to these questions, numerical simulations are a powerful method to reveal the influence of coated microphysics on its SAE, which is generally missing.

Here, numerical investigations of the SAE of polydisperse BC aggregates coated by organics are systematically carried out based on current understanding. An accurate multiple-sphere T-matrix method (MSTM) is applied to calculate scattering properties of coated BC at several incident wavelengths and then its SAE. The aim is to assess the influences of particle microphysical configurations, including shell/core ratio, BC geometry, coated volume fraction of BC, and size distribution, on the SAE of coated BC particles, which hopefully benefits our understanding of aerosol SAE and its further applications.

2. Methodology: BC models and numerical simulation

Fresh BC is usually loose chain -like aggregate with plenty of similar-sized near-spherical monomers, and the fractal aggregate is mathematically utilized to construct BC geometries following:

$$N = \mathrm{k}_0\left(\frac{R_g}{a}\right)^{D_f}, \tag{1}$$

$$R_g = \sqrt{\frac{1}{N}\sum_{i=1}^{N} r_i^2}, \tag{2}$$

where the monomer number (N), fractal prefactor (k_0), gyration radius (R_g), monomer radius (a), and fractal dimension (D_f) construct an aggregate [e.g., 15]. The D_f of fresh BC is commonly smaller than 2, whereas it can be near 3 for aged BC due to collapse induced by coating of secondary organic aerosols during aging process [e.g., 16]. For aged BC, the coated volume fraction of BC (F) is a parameter applied to describe BC coating state, and it can be given in the form of

$$F = \frac{V_{BCinside}}{V_{BC}}, \tag{3}$$

where $V_{BCinside}$ and V_{BC} are volume of BC monomers inside coating and volume of overall BC aggregate, respectively. With this definition, externally attached, partially coated, and fully coated BC aggregates show $F = 0$, $0 < F < 1$, and $F = 1$, respectively.

To construct the model of aged BC, spherical organics is assumed to coat BC aggregates following Zhang et al. [17]. BC aggregate is generated with a tunable particle-cluster aggregation algorithm from Skorupski et al. [18]. The D_f values of BC aggregates are assumed as 1.8 and 2.8, which represent lacy and compact BC, respectively [19], while the k_0 is assumed as 1.2 [14]. we consider N of 200, as ambient BC is mostly in accumulation mode following Zhang and Mao [20]. After BC aggregate generated, a spherical organics is put to coat BC aggregate with expected F values. Note that some BC monomers are mildly shifted to avoid overlapping, resulting in a slight variation of BC D_f, whereas the geometry of aggregate is still maintained. The sketch maps of constructed coated BC models are shown in Fig. 1 following Zhang et al. [21].

Table 1
Key microphysical properties of coated BC aggregates.

Parameter		applied values
F		0.0, 0.25, 0.5, 0.75, 1.0
D_p/D_c		1.1, 1.5, 1.9, 2.3, 2.7
BC D_f		1.8, 2.8
Size distribution	r_g, μm	0.075 (0.05–0.15)
	σ_g	1.59

Table 2
Definitions of key microphysical parameters of coated BC aggregates.

Parameter	definition
F	coated volume fraction of BC
D_p/D_c	spherical equivalent particle diameter divided by BC core diameter
D_f	fractal dimension of BC aggregate

The optical properties of modelled coated BC are calculated with the multiple-sphere T-matrix method [22], and this exactly numerical method is widely utilized for various investigations BC properties [e.g., 23]. This study considers coated BC following lognormal size distributions, as bulk aerosol properties are meaningful for ambient applications. Applied lognormal size distribution is in form of

$$\mathrm{n}(r) = \frac{1}{\sqrt{2\pi}\, r \ln(\sigma_g)} \exp\left[-\left(\frac{\ln(r) - \ln(r_g)}{\sqrt{2}\ln(\sigma_g)}\right)^2\right], \tag{4}$$

where σ_g and r_g are geometric standard deviation, and geometric mean radius, respectively [e.g., 24]. As coated BC in accumulation mode is considered, the size range is set as 0.1–1 μm while r_g of 0.075 μm and σ_g of 1.59 are assumed [25]. Given size distribution, bulk scattering cross sections of coated BC are calculated with the equation following

$$\langle C_{sca}\rangle = \int_{r_{\min}}^{r_{\max}} C_{sca}(r) n(r) d(r) \tag{5}$$

Scattering Angstrom exponent can be applied to express the scattering dependence on wavelength, and conventionally, the SAE at two wavelengths λ_1 and λ_2 can be described explicitly as

$$SAE(\lambda_1, \lambda_2) = -\frac{\ln(\langle C_{sca}(\lambda_1)\rangle) - \ln(\langle C_{sca}(\lambda_2)\rangle)}{\ln(\lambda_1) - \ln(\lambda_2)}. \tag{6}$$

Obviously, the SAE is the negative slope of coated BC scattering between incident wavelength λ_1 and λ_2 on a log-log scale [e.g., 11].

The SAE of BC coated by non-absorbing organics is studied at incident wavelengths of 450 nm, 550 nm and 700 nm. The refractive indices of BC and non-absorbing organics are assumedly wavelength-independent with values of $1.85 - 0.71i$ [26], and $1.55 - 0i$ [27], respectively for considered wavelengths. The BC shell/core ratio D_p/D_c is spherical equivalent particle diameter divided by BC core diameter (D_c), and is assumed in a range of 1.1–2.7 [28,29]. BC key microphysical parameters considered and their definitions are summarized in Table 1 and 2, respectively. Note that some SAE results of coated BC with small D_p/D_c and large F cannot be shown, because F, D_p/D_c and BC D_f restrict each other in a

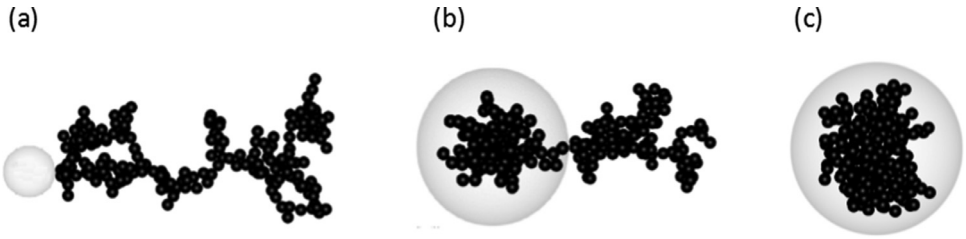

Fig. 1. Sketch maps of geometries of coated BC with BC aggregates containing 200 monomers based on Zhang et al. [21]. The fractal BC aggregates are externally attached to organics with $F = 0.0$ (a), as well as partially coated BC with $F = 0.5$ (b), and BC fully encapsulated in organics with $F = 1.0$ (c).

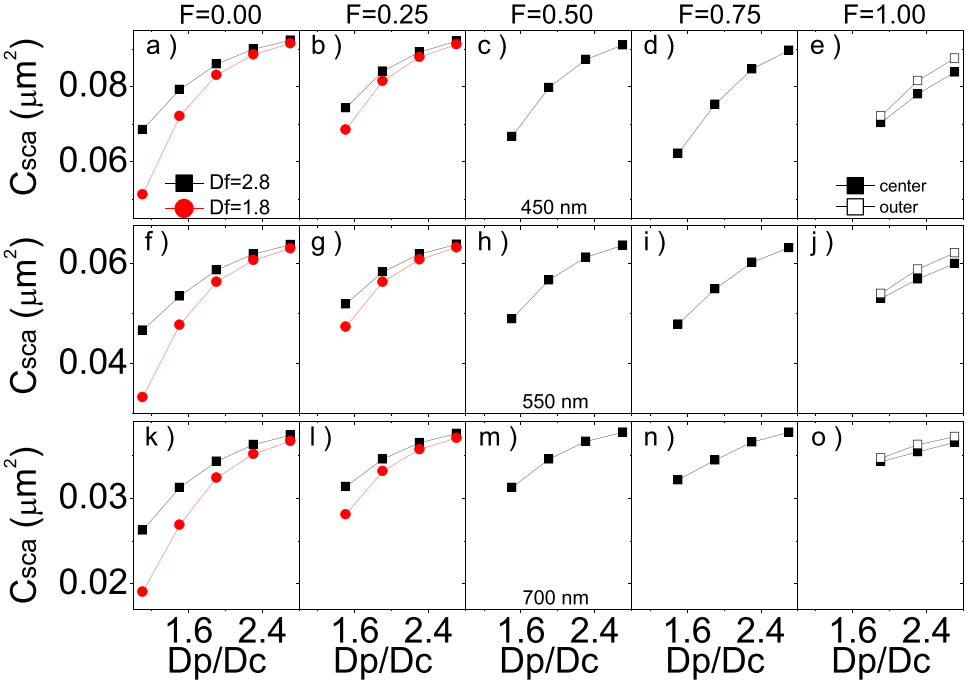

Fig. 2. Scattering cross sections (C_{sca}) of coated BC as a function of shell/core ratio (Dp/Dc) at 350 nm (upper row), 550 nm (middle row), and 700 nm (bottom row). Coated volume fractions of BC (F) of 0.00, 0.25, 0.5, 0.75, and 1.00 are considered (from left to right). Black squares and red circles indicate BC D_f of 2.8 and 1.8, respectively. For $F = 1.0$, black solid squares indicate BC aggregates at particle geometric center, whereas black open squares denote BC at an outmost position close to coating boundary.

fixed coated BC particle. With more realistic coated BC models defined, the impact of detailed coated BC microphysics on its SAE is investigated as follows.

3. Results and discussion

3.1. Scattering properties of coated BC at a single wavelength

Fig. 2 illustrates scattering cross sections of coated BC at three wavelengths of 450 nm, 550 nm and 700 nm at different shell/core ratios. Five coated volume fractions of BC with $F = 0.0$, 0.25, 0.5, 0.75 and 1.0 and two BC fractal dimensions with $D_f = 1.8$ and 2.8 are considered. The scattering properties are averaged over coated BC ensembles with the aforementioned size distribution. As shown in Fig. 2, scattering cross sections of coated BC are dependent on shell/core ratio, coated volume fraction of BC, BC position inside coating, and BC fractal dimension. Among all four BC microphysical parameters, the dependence of scattering cross sections of coated BC on shell/core ratio is highest, indicating the significance of BC shell/core ratio measurement in ambient air. Starting from incident wavelength of 550 nm, as D_p/D_c increases from 1.1 to 2.7, the C_{sca} of externally attached BC with a BC D_f of 2.8 increases from ~0.05 μm^2 to ~0.06 μm^2. With BC becoming fully coated, their C_{sca} values at 550 nm also vary in a range of ~0.05 μm^2 to ~0.06 μm^2, as D_p/D_c changes from 1.9 to 2.7. For a fixed BC D_f, the C_{sca} generally decreases slightly, as F increases from 0 to 1. This is owing to that the coating of non-absorbing organics suppresses the contribution of BC aggregate core to scattering cross section of coated BC. In addition to D_p/D_c and F, the C_{sca} is also sensitive to BC geometry, and the sensitivity of C_{sca} to BC geometry becomes weaker as D_p/D_c and F become larger. When BC aggregates become compact, i.e., increased D_f, the C_{sca} of coated BC with fixed D_p/D_c and F becomes large, and this is consistent with the bare BC results of Liu et al. [15]. For fully coated BC, the C_{sca} of coated BC with an outmost off-center core-shell structure is slightly higher than that given by the concentric core-shell structure. With increased incident wavelength, the C_{sca} of coated BC decreases, indicating positive scattering Angstrom exponent, which will be discussed in following subsection.

3.2. Scattering Angstrom exponent of coated BC

With scattering properties at various wavelengths, the SAE of coated BC can be obtained based on their scattering cross sections

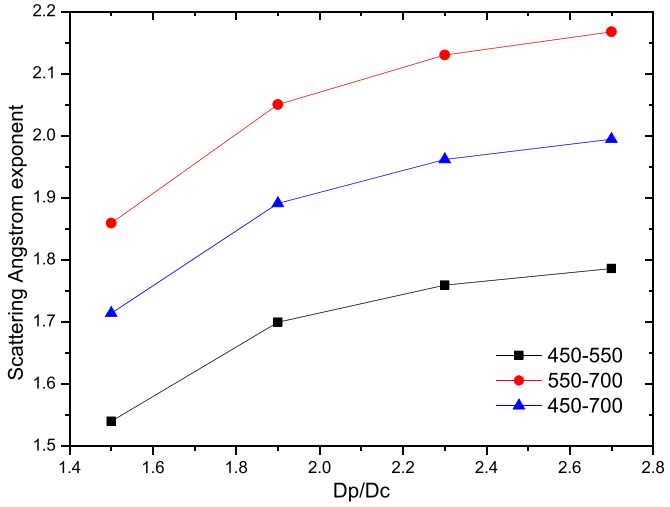

Fig. 3. Scattering Angstrom exponent of coated BC at different wavelengths as a function of shell/core ratio (Dp/Dc). Coated BC with coated volume fraction of BC of 0.5 and BC D_f of 2.8 is considered as an example.

at wavelengths of 450 nm and 700 nm, and the $SAE_{450-550}$ and $SAE_{550-700}$, referring to values between wavelengths of 450 nm and 550 nm and between 550 nm and 700 nm, are also considered for comparison. Fig. 3 shows scattering Angstrom exponents of coated BC with a F of 0.5, and BC D_f of 2.8 based on different wavelength selections. One can see that the SAE between smaller wavelengths has smaller values, and the SAE between wavelengths of 450 nm and 700 nm have moderate value. The wavelength selection can result in SAE uncertainty within 10%, and we consider SAE between wavelengths of 450 nm and 700 nm for further investigations of the SAE impacted by coated BC microphysics.

Fig. 4 illustrates the SAE of coated BC with the aforementioned size distribution, and the SAE is calculated based on wavelengths of 450 nm and 700 nm. It is clear to see that the SAE of coated BC is sensitive to BC fractal dimension, BC position inside coating, coated volume fraction of BC, and shell/core ratio. The SAE of coated BC varies in ranges of 2.0–2.2, 1.9–2.0, 1.7–2.0, 1.5–2.0 and 1.6–1.9 for $F = 0.0$, 0.25, 0.5, 0.75 and 1.0, respectively. The SAE of coated BC increases with increased D_p/D_c for $F \geq 0.5$, as opposed to a decrease of the SAE for externally attached BC. For fixed D_p/D_c and BC D_f, the SAE of coated BC decreases along with the increase of F, indicating more BC coated in non-absorbing organics can reduce the SAE. This is probably related to the fraction volume-equivalent size parameter that is covered by absorbing versus non-absorbing medium. More BC coated in non-absorbing organics reduces coated BC scattering due to the suppression of scattering contribution of BC core by the coating [30]. The SAE shows mildly sensitive to BC D_f, and more compact BC leads to smaller coated BC SAE. BC position inside coating can also affect the SAE, and coated BC with BC at an outer position within coating has large SAE. In addition to single effects, coated BC microphysics has comprehensive effects its SAE. With increased F, the SAE of coated BC becomes less sensitive to BC D_f, but more sensitive to D_p/D_c, i.e., showing larger variation.

In addition to BC microphysics (i.e., BC fractal dimension, BC position inside coating, coated volume fraction of BC, and shell/core ratio) considered above, we also study the impacts of the distributions of BC geometry shape and coated volume fraction of BC on the SAE of coated BC. Fig. 5 illustrates the SAE of coated BC with the aforementioned size distribution between 450 nm and 700 nm as functions of shell/core ratio and percentage of compact BC. The percentage of compact BC is the fraction of coated BC with BC D_f of 2.8 among all considered coated BC particles including BC D_f values of both 1.8 and 2.8, and the SAE results for coated BC with F of 0.0 and 0.25 are shown from top to bottom in Fig. 5. It is clearly that the SAE of coated BC decreases with increased percentage of compact BC particles, indicating that more compact BC leads to smaller SAE of coated BC. The influence of the distribution of coated volume fraction of BC on the SAE of coated BC with BC D_f of 2.8 is illustrated in Fig. 6. Coated BC follows the aforementioned fixed size distribution, and F values of 0.0, 0.5 and 1.0 are con-

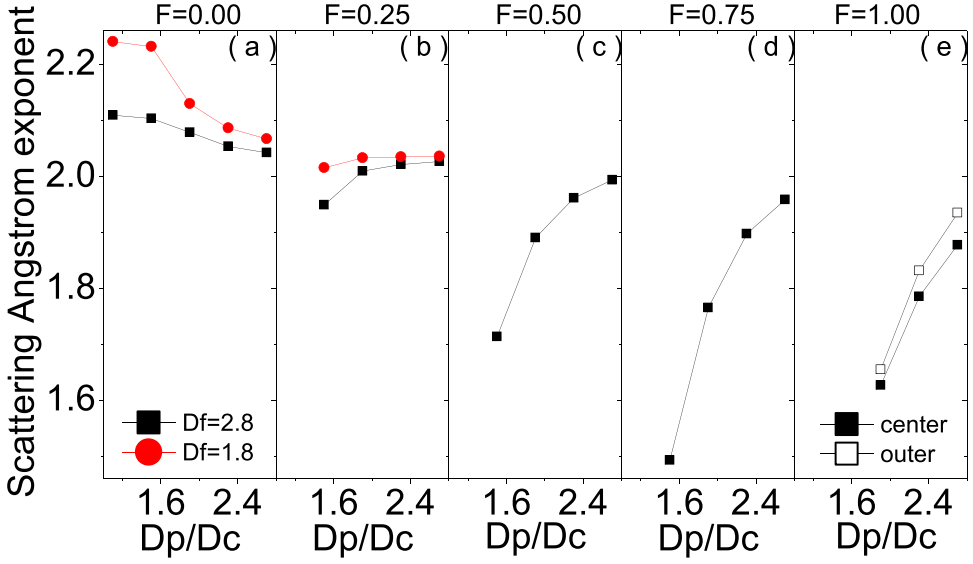

Fig. 4. Scattering Angstrom exponent of coated BC as a function of shell/core ratio (Dp/Dc). Coated volume fractions of BC (F) of 0.00, 0.25, 0.5, 0.75, and 1.00 are considered (from left to right). Black squares and red circles indicate BC D_f of 2.8 and 1.8, respectively. For $F = 1.0$, black solid squares indicate BC aggregates at particle geometric center, whereas black open squares denote BC at an outmost position close to coating boundary.

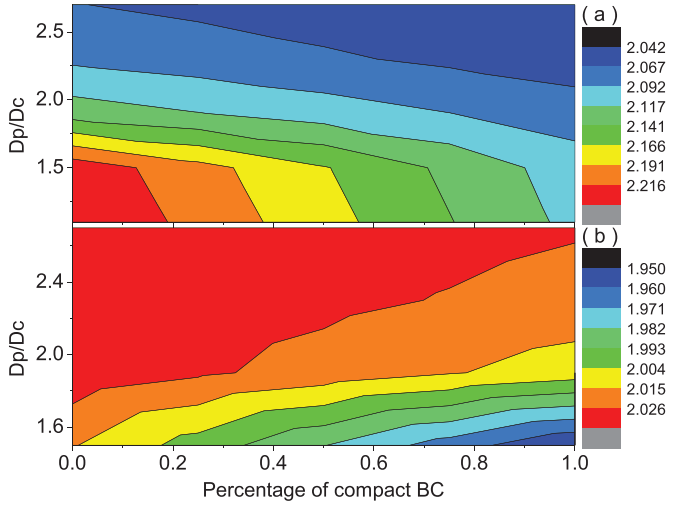

Fig. 5. Scattering Angstrom exponent of coated BC as functions of shell/core ratio (Dp/Dc) and percentage of compact BC (Df = 2.8) among coated BC with BC Df values of 1.8 and 2.8. Coated volume fractions of BC of 0.0 (a) and 0.25 (b) are considered.

sidered for the F distribution. We can see that coated BC particles with more percentage of $F = 0.0$ or less fraction of $F = 1.0$ show larger SAE values for all considered shell/core ratios. This indicates that more externally attached BC structures or less fully coated BC structures result in larger SAE of coated BC.

Fig. 7 shows the SAE variations for coated BC (BC fractal dimension of 2.8) with different particle size distributions and shell/core ratios. The panels in Fig. 7 from left to right correspond to coated volume fractions of BC with $F = 0.0$, 0.5 and 1.0, and a concentric spherical core-shell structure. Again, the SAE is obtained on the basis of wavelengths of 450 nm and 700 nm, and lognormal size distributions are assumed for coated BC with r_g (x axis) ranging from 0.05–0.15 μm and σ_g fixed as 1.59. As shown in Fig. 7, the SAE of coated BC shows broad variations with values in ranges of 0.9–2.6, 0.8–2.6 and 0.5–2.5 for $F = 0.0$, 0.5 and 1.0, respectively. Meanwhile, most of SAE values obtained for aged BC particles are less than 2.0, and this can potentially explain observed relatively small SAE values in ambient air [e.g., 31–33]. The coated BC SAE is highly sensitive to size distribution, and for fixed F and D_p/D_c, it decreases as r_g increases, i.e., particle becoming larger. Compared to F and D_p/D_c, the dependence of the SAE on size distribution is significantly stronger. This demonstrates that the SAE is a parameter depending primarily on particle size. However, other coated BC microphysical parameters, such as F and D_p/D_c, can also have some impacts on its SAE. For instance, the dependence of the SAE on D_p/D_c becomes close to the dependence on size distribution for thinly coated BC (i.e., small D_p/D_c). This indicates that smaller SAE may not always be indicative of more large particles, especially for thinly coated BC, due to the influences of other particle microphysics. Compared to more realistic BC geometries, the concentric spherical core-shell structure generally produces acceptable SAE results for heavily coated BC (differences within 10%), whereas significant SAE errors can be induced for thinly coated BC particles.

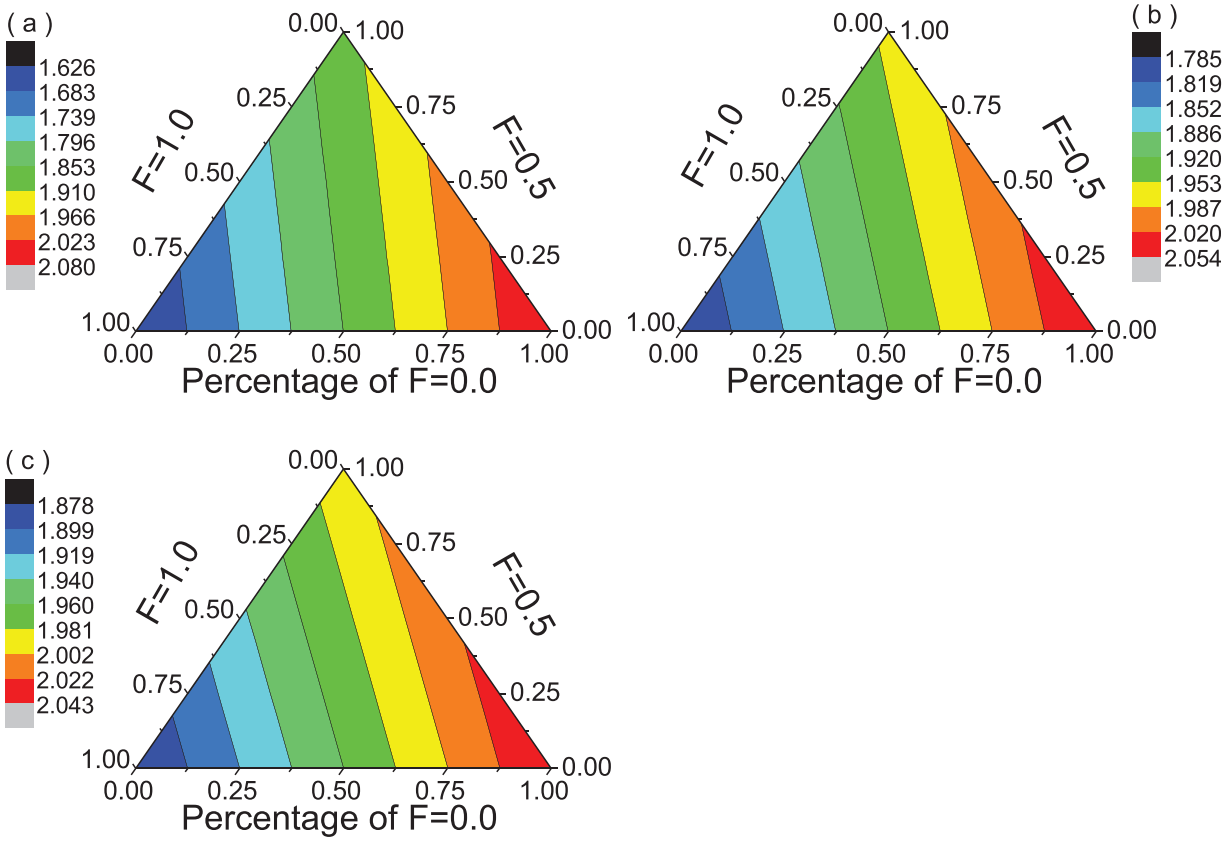

Fig. 6. Scattering Angstrom exponent of coated BC as a function of coated volume fraction of BC distribution for shell/core ratios of 1.9 (a), 2.3 (b) and 2.7 (c). Percentages of coated volume fractions of BC (F) of 0.0, 0.5 and 1.0 are considered for the F distribution. BC Df of 2.8 is considered, and for $F = 1.0$, BC aggregates are at particle geometric center.

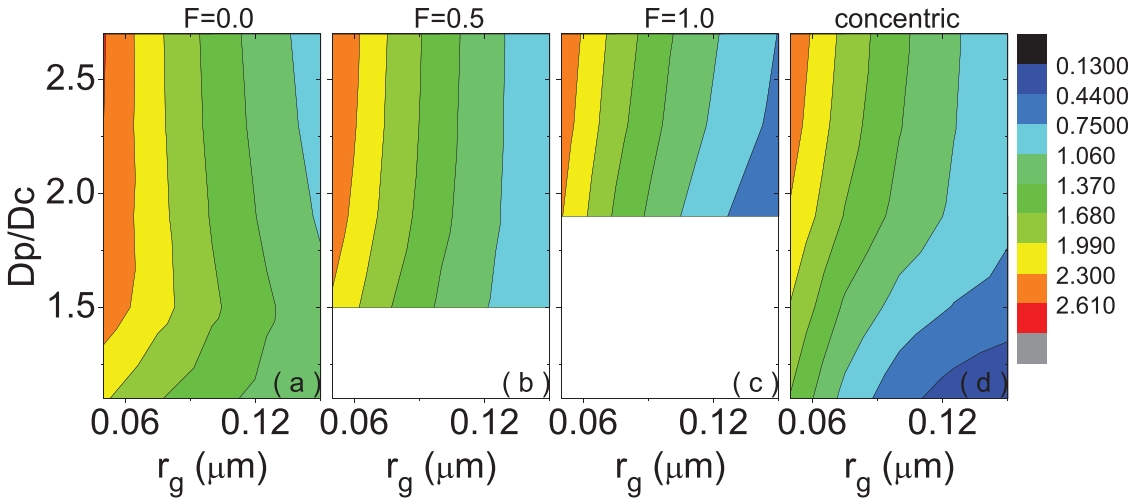

Fig. 7. Scattering Angstrom exponent of coated BC (BC D_f of 2.8) with different shell/core ratio (Dp/Dc) and particle size distribution. Three coated volume fractions of BC, i.e., 0.00, 0.50, and 1.00, as well as spherical concentric core-shell, are shown from left to right. For fully coated BC structure, BC is located at particle geometric center. The geometric standard deviations (σ_g) for applied lognormal distribution are 1.59.

4. Conclusions

This study investigates the influences of shell/core ratio, BC geometry, coated volume fraction of BC, and size distribution on the SAE of coated BC aerosols. Realistic BC geometry is modelled by the fractal aggregate, and coated BC SAE is calculated based on the MSTM method. Our results indicate that among all microphysical parameters, the dependence of coated BC scattering on shell/core ratio is important, indicating the significance of BC shell/core ratio measurement in the atmosphere. The SAE of coated BC shows wavelength dependence with smaller value at smaller wavelength, whereas the SAE differences due to wavelength selection are within 10%. The SAE of coated BC between 450 nm and 700 nm shows broad variation with a range of 0.5–2.6 for typical coated BC microphysics. Our study demonstrates that the SAE of coated BC is highly sensitive to particle size distribution, and for fixed F, BC D_f and D_p/D_c, it decreases with particle becoming larger. Compared to size distribution, the dependence of the SAE on other coated BC microphysics (such as F or D_p/D_c) is generally weak, and the SAE of coated BC with larger F becomes less sensitive to BC D_f but more sensitive to D_p/D_c. Nevertheless, smaller SAE of coated BC may not always indicates larger particles, especially for thinly coated BC, and the dependence of their SAE on D_p/D_c becomes close to the dependence on size distribution. The popular core-shell Mie model generally gives acceptable SAE results for heavily coated BC with differences within 10%, while significant SAE errors can be introduced for thinly coated BC particles. Overall, this work clearly demonstrates the impact of particle size distribution on the SAE of coated BC based on more realistic BC geometries. However, caution should be taken in interpreting the SAE values as an absolute reference to particle size, particularly for thinly coated BC aerosols. Furthermore, there still remains a fair amount of parameter-unification, such as q-space [34], and the ratio of light penetration depth to particle size is likely to provide a quasi-wavelength-independent view of SAE affected by aerosol microphysics [e.g., 35], which will be our further works.

Author statement

M. Mao and X. Zhang conceived the research plan. X. Zhang performed the simulations and wrote the manuscript. All authors discussed the results and contributed the final paper.

Declaration of Competing Interest

The authors declare that they have no conflict of interest.

Acknowledgments

This work is financially supported by the National Natural Science Foundation of China (NSFC) (41505127), and Natural Science Foundation of Jiangsu Province (BK20150901). This work is also supported by the Key Laboratory of Middle Atmosphere and Global Environment Observation (LAGEO-2019-04), and Key Laboratory of Meteorological Disaster, Ministry of Education (KLME201810). We particularly acknowledge the source of the codes of MSTM 3.0 from Daniel W. Mackowski.

References

[1] Myhre G. Consistency between satellite-derived and modeled estimates of the direct aerosol effect. Science 2009;325(5937):187–90.
[2] Ramanathan V, Carmichael G. Global and regional climate changes due to black carbon. Nat. Geosci. 2008;1(4):221–7.
[3] Intergovernmental Panel on Climate Change (IPCC). Climate Change 2013: The Physical Science Basis. Cambridge University Press, UK.
[4] Schnaiter M. Absorption amplification of black carbon internally mixed with secondary organic aerosol. J. Geophys. Res. 2005;110(D19):D19204.
[5] Shiraiwa M, Kondo Y, Iwamoto T, Kita K. Amplification of light absorption of black carbon by organic coating. Aerosol. Sci. Technol. 2010;44(1):46–54.
[6] Bond TC, J Doherty S, Fahey DW, Forster PM, Berntsen T, DeAngelo BJ, Flanner MG, Ghan S, Kaercher B, Koch D, Kinne S, Kondo Y, Quinn PK, Sarofim MC, Schultz MG, Schulz M, Venkataraman C, Zhang H, Zhang S, Bellouin N, Guttikunda SK, Hopke PK, Jacobson MZ, Kaiser JW, Klimont Z, Lohmann U, Schwarz JP, Shindell D, Storelvmo T, Warren SG, Zender CS. Bounding the role of black carbon in the climate system: a scientific assessment. J. Geophys. Res. 2013;118(11):5380–552.
[7] Costabile F, Barnaba F, Angelini F, Gobbi GP. Identification of key aerosol populations through their size and composition resolved spectral scattering and absorption. Atmos. Chem. Phys. 2013;13:2455–70.
[8] Kaskaoutis DG, Kambezidis HD. Comparison of the Angstrom parameters retrieval in different spectral ranges with the use of different techniques. Meteorol. Atmos Phys. 2008;99:233–46.
[9] Russell PB, Bergstrom RW, Shinozuka Y, Clarke AD, DeCarlo PF, Jimenez JL, Livingston JM, Redemann J, Dubovik O, Strawa A. Absorption angstrom exponent in AERONET and related data as an indicator of aerosol composition. Atmos Chem. Phys. 2010;10:1155–69.
[10] Lack DA, Cappa CD. Impact of brown and clear carbon on light absorption enhancement, single scatter albedo and absorption wavelength dependence of black carbon. Atmos Chem. Phys. 2010;10:4207–20.
[11] Moosmuller H, Chakrabarty RK. Technical note: simple analytical relationships between Angstrom coefficients of aerosol extinction, scattering, absorption, and single scattering albedo. Atmos Chem. Phys. 2011;11:10677–10680.

[12] Cappa CD, Onasch TB, Massoli P, Worsnop DR, Bates TS, Cross ES, Davidovits P, Hakala J, Hayden KL, Jobson BT, Kolesar KR, Lack DA, Lerner BM, Li SM, Mellon D, Nuaaman I, Olfert JS, Petaja T, Quinn PK, Song C, Subramanian R, Williams EJ, Zaveri RA. Radiative absorption enhancements due to the mixing state of atmospheric black carbon. Science 2012;337:1078–81.
[13] Zhang X, Mao M. Radiative properties of coated black carbon aerosols impacted by their microphysics. J. Quant. Spectrosc. Radiat. Transf. 2020;241:106718.
[14] Luo J, Zhang Y, Wang F, Zhang Q. Effects of brown coatings on the absorption enhancement of black carbon: a numerical investigation. Atmos. Chem. Phys. 2018;18:16897–914.
[15] Sorensen CM. Light scattering by fractal aggregates: a review. Aerosol. Sci. Technol. 2001;35(2):648–87.
[16] Tritscher T, Juranyi Z, Martin M, Chirico R, Gysel M, Heringa MF, DeCarlo PF, Sierau B, Prevot ASH, Weingartner E, Baltensperger U. Changes of hygroscopicity and morphology during ageing of diesel soot. Environ. Res. Lett. 2011;6:034026.
[17] Zhang X, Mao M, Yin Y, Wang B. Numerical investigation on absorption enhancement of black carbon aerosols partially coated with nonabsorbing organics. J. Geophys. Res. 2018;123:1297–308.
[18] Skorupski K, Mroczka J, Wriedt T, Riefler N. A fast and accurate implementation of tunable algorithms used for generation of fractal-like aggregate models. Physica A 2014;404:106–17.
[19] Wu Y, Cheng TH, Zheng LJ, Chen H. Optical properties of the semi-external mixture composed of sulfate particle and different quantities of soot aggregates. J. Quant. Spectrosc. Radiat. Transf. 2016;179:139–48.
[20] Zhang X, Mao M, Yin Y. Optically effective complex refractive index of coated black carbon aerosols: from numerical aspects. Atmos. Chem. Phys. 2019;19:7507–18.
[21] Zhang X, Mao M, Yin Y, Tang S. The absorption Angstrom exponent of black carbon with brown coatings: effects of aerosol microphysics and parameterization. Atmos. Chem. Phys. 2020;20:9701–11.
[22] Mackowski DW. A general superposition solution for electromagnetic scattering by multiple spherical domains of optically active media. J. Quant. Spectrosc. Radiat. Transf. 2014;133:264–70.
[23] Mishchenko MI, Dlugach JM, Yurkin MA, Bi L, Cairns B, Liu L, Panetta LR, TravisL Yang P, Zakharova N. First-principles modeling of electromagnetic scattering by discrete and discretely heterogeneous random media. Phys. Rep. 2016;632:1–75.
[24] Zhang X, Mao M, Chen H. Characterization of optically effective complex refractive index of black carbon composite aerosols. J. Atmos Sol.-Terr. Phy. 2020;198:105180.
[25] Zhang K, O'Donnell D, Kazil J, Stier P, Kinne S, Lohmann U, Ferrachat S, Croft B, Quaas J, Wan H, Rast S, Feichter J. The global aerosol-climate model ECHAM-HAM, version 2: sensitivity to improvements in process representations. Atmos. Chem. Phys. 2012;12:8911–49.
[26] Bond TC, Bergstrom RW. Light absorption by carbonaceous particles: an investigative review. Aerosol. Sci. Technol. 2006;40:27–67.
[27] Chakrabarty RK, Moosmuller H, Chen LWA, Lewis K, Arnott WP, Mazzoleni C, Dubey MK, Wold CE, Hao WM, Kreidenweis SM. Brown carbon in tar balls from smoldering biomass combustion. Atmos. Chem. Phys. 2010;10(13):6363–6370.
[28] Liu D, Taylor JW, Young DE, Flynn MJ, Coe H, Allan JD. The effect of complex black carbon microphysics on the determination of the optical properties of brown carbon. Geophys. Res. Lett. 2015;42:613–19.
[29] Zhang Y, Zhang Q, Cheng Y, Su H, Kecorius S, Wang Z, Wu Z, Hu M, Zhu T, Wiedensohler A, He K. Measuring the morphology and density of internally mixed black carbon with SP2 and VTDMA: new insight into the absorption enhancement of black carbon in the atmosphere. Atmos. Meas. Tech. 2016;9:1833–43.
[30] Mishchenko MI, Dlugach JM. Adhesion of mineral and soot aerosols can strongly affect their scattering and absorption properties. Opt. Lett. 2012;37:704–6.
[31] Kim SW, Yoon SC, Jefferson A, Ogren JA, Dutton EG, Won JG, Ghim YS, Lee BI, Han JS. Aerosol optical, chemical and physical properties at Gosan, Korea during Asian dust and pollution episodes in 2001. Atmos. Environ. 2005;39:39–50.
[32] Yang M, Howell SG, Zhuang J, Huebert BJ. Attribution of aerosol light absorption to black carbon, brown carbon, and dust in China — interpretations of atmospheric measurements during EAST-AIRE. Atmos. Chem. Phys. 2009;9:2035–50.
[33] Valenzuela A, Olmo FJ, Lyamani H, Anton M, Titos G, Cazorla A, Alados-Arboledas L. Aerosol scattering and absorption Angstrom exponents as indicators of dust and dust-free days over Granada (Spain). Atmos. Res. 2015;154:1–13.
[34] Sorensen CM. Q-space analysis of scattering by particles: a review. J. Quant. Spectrosc. Radiat. Transf. 2013;131:3–12.
[35] Piedra PG, Moosmuller H. Optical losses of photovoltaic cells due to aerosol deposition: role of particle refractive index and size. Solar Energy 2017;155:637–46.